OFFPRINT

Driven polymer translocation through nanopores: Slow-vs.-fast dynamics

K. Luo, T. Ala-Nissila, S.-C. Ying and R. Metzler

Please visit the new website
www.epljournal.org

TARGET YOUR RESEARCH WITH EPL

Sign up to receive the free EPL table of contents alert.

www.epljournal.org/alerts

Driven polymer translocation through nanopores: Slow-vs.-fast dynamics

K. Luo[1,2(a)], T. Ala-Nissila[3,4], S.-C. Ying[4] and R. Metzler[1]

[1] *Physics Department, Technical University of Munich - D-85748 Garching, Germany, EU*
[2] *Department of Polymer Science and Engineering and CAS Key Laboratory of Soft Matter Chemistry*
University of Science and Technology of China - Hefei, Anhui 230026, China
[3] *Department of Applied Physics and COMP Center of Excellence, Helsinki University of Technology*
P.O. Box 1100, FIN-02015 TKK, Espoo, Finland, EU
[4] *Department of Physics, Brown University, P.O. Box 1843, Providence, RI 02912, USA*

Abstract – We investigate the dynamics of polymer translocation through nanopores under external driving by 3D Langevin Dynamics simulations, focusing on the scaling of the average translocation time τ *vs.* the length of the polymer, $\tau \sim N^{\alpha}$. For slow translocation, *i.e.*, under low driving force and/or high friction, we find $\alpha \approx 1 + \nu \approx 1.588$, where ν denotes the Flory exponent. In contrast, $\alpha \approx 1.37$ is observed for fast translocation due to the highly deformed chain conformation on the trans side, reflecting a pronounced non-equilibrium situation. The dependence of the translocation time on the driving force is given by $\tau \sim F^{-1}$ and $\tau \sim F^{-0.80}$ for slow and fast translocation, respectively. These results clarify the controversy on the magnitude of the scaling exponent α for driven translocation.

Introduction. – The passage of a polymer through a nanopore is essential for numerous biological processes such as DNA and RNA translocation across nuclear pores, protein transport through membrane channels, or virus injection into cells [1]. (Bio)polymer translocation is also at the heart of various potential technology applications, for instance, rapid DNA sequencing, gene therapy, or controlled drug delivery [2]. A translocating polymer has to overcome an entropic barrier. In biological cells, biopolymers are driven through pores by transmembrane potentials, chemical potential gradients due to binding proteins, active pulling by polymerase, or entropic pressure (virus ejection) [1]. From both the basic physics as well as a technology design perspective, an important measure is the scaling of the average translocation time τ with the polymer length N, $\tau \sim N^{\alpha}$, and the value of the corresponding scaling exponent α.

Most translocation experiments are carried out under an applied electric field across the pore. We focus here on this particular type of driven translocation. In experiments with α-hemolysin pores of inner diameter 2 nm a linear behavior of $\tau \sim N$ ($\alpha = 1$) was observed [3,4], while an exponent $\alpha = 1.27$ was obtained for double-stranded DNA translocation through a solid-state nanopore of inner diameter 10 nm [5]. Recently the voltage-driven translocation of individual DNA molecules through solid-state nanopores of diameters $2.7 \ldots 5$ nm revealed that $\tau \sim N^{1.40}$ for DNA molecules in the range 150–3500 base pairs [6].

Inspired by these experiments, a number of recent theories and simulations on the translocation dynamics have been presented. Standard Kramers analysis of diffusion across an equilibrium entropic barrier yields $\tau \sim N^2$ for unbiased translocation and $\tau \sim N$ under external driving (assuming friction to be N-independent) [7,8]. However, as noted in ref. [9] the quadratic scaling behavior in the unbiased case cannot be correct for a self-avoiding polymer, as the translocation time would be shorter than the Rouse equilibration time scaling like $\tau_R \sim N^{1+2\nu}$, involving the Flory exponent ν ($\nu = 0.588$ in 3D, $\nu = 0.75$ in 2D) [10]. This finding renders the concept of equilibrium entropy and the ensuing picture of entropic barrier crossing inappropriate for translocation dynamics. Numerically,

(a)E-mail: luokaifu@gmail.com

it was shown that for large N, $\tau \sim N^{1+2\nu}$, *i.e.*, the translocation time scales in the same way as the equilibration time, but with a much larger prefactor [9]. This result was recently corroborated by extensive numerical simulations based on the Fluctuating Bond (FB) [11] and Langevin Dynamics (LD) models with the bead-spring approach [12–14]. For *driven* translocation, the deviation from equilibrium is expected to be even more pronounced, and the equilibrium entropic barrier is less relevant for the translocation dynamics. For this case, a lower bound $\tau \sim N^{1+\nu}$ was estimated for the translocation time [15]. Lattice Monte Carlo (MC) simulations of self-avoiding chains in $2D$ revealed $\alpha \approx 1.5$ [15], which is smaller than $1+\nu = 1.75$, a difference attributed to finite-size effects. However, additional simulation studies found a crossover from $\tau \sim N^{1.46\pm0.01} \approx N^{2\nu}$ for relatively short polymers to $\tau \sim N^{1.70\pm0.03} \approx N^{1+\nu}$ for longer chains ($N > 200$) using FB [16] and LD [12,17] models in 2D. Increasing the friction, the crossover vanished and only exponent $1+\nu$ was observed [12]. However, the crossover is absent in 3D for quite long chains ($N \sim 800$) and $\alpha \approx 1.40$ is observed using both LD [18] and GROMACS molecular dynamics with LD thermostats [19] simulations. Lehtola *et al.* [20] find approximately the same exponent of about 1.40 based on LD simulations, however, their exponent increases with increasing force, which cannot hold asymptotically. Moreover, Gauthier and Slater [21] reported $\tau \sim N^{1+\nu}$ using an exact numerical method valid at low bias.

Recently, however, alternative scaling scenarios have been presented in refs. [22,23] that contradict above results. These two views disagree with each other [24]. To resolve the apparent discrepancy on the value of α for driven translocation, we here report results on the behavior of τ as a function of N from high-accuracy LD simulations in 3D. As in the above-mentioned studies, we also neglect hydrodynamics effects as well as polymer-pore interactions [25]. We find that there exists two limiting regimes, corresponding to slow and fast translocation, respectively. The slow translocation case is realized for low driving forces and/or high friction, and in this regime $\alpha \approx 1+\nu$. In the opposite limit of fast translocation for high driving forces and/or low friction, the corresponding scaling exponent is given by $\alpha \approx 1.37$. As we will argue below, the difference between the scaling exponents for these two regimes can be ascribed to the highly deformed chain conformation during fast translocation, reflecting a pronounced non-equilibrium situation. Our results clarify the controversy on the value of α for driven translocation.

Model and method. – In our simulations, the polymer chains are modeled as bead-spring chains of Lennard-Jones (LJ) particles with the Finite Extension Nonlinear Elastic (FENE) potential. Excluded-volume interaction between monomers is modeled by a short range repulsive LJ potential: $U_{LJ}(r) = 4\varepsilon[(\frac{\sigma}{r})^{12} - (\frac{\sigma}{r})^6] + \varepsilon$ for $r \leqslant 2^{1/6}\sigma$, and 0 for $r > 2^{1/6}\sigma$. Here, σ is the monomer diameter and ε is the potential depth. The connectivity between
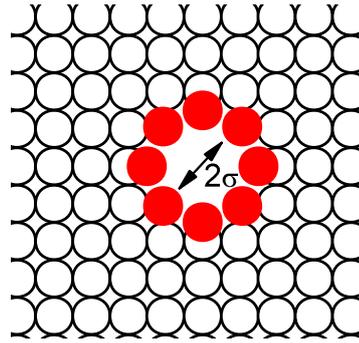

Fig. 1: (Colour on-line) Schematic representation of our simulation system. The wall consists in a single layer of beads while the pore itself is formed by eight particles with their centers equally distributed on a circle of diameter 3σ. Therefore, the actual pore diameter is 2σ.

neighboring monomers is modeled as a FENE spring with $U_{FENE}(r) = -\frac{1}{2}kR_0^2\ln(1 - r^2/R_0^2)$, where r is the distance between consecutive monomers, k the spring constant, and R_0 the maximum allowed separation between connected monomers. The wall ("membrane") carrying the pore is composed of particles of diameter σ. The wall thickness is σ. The nanopore consists of eight particles with their centers equally distributed on a circle of diameter 3σ, see fig. 1. Therefore, the actual pore diameter is 2σ. Between all monomer-wall particle pairs, there exists the same short range repulsive LJ interaction as described above.

In LD simulations each monomer is subjected to conservative, frictional, and random forces: $m\ddot{\mathbf{r}}_i = -\boldsymbol{\nabla}(U_{LJ} + U_{FENE}) - \xi\dot{\mathbf{r}}_i + \mathbf{F}_{\text{ext}} + \mathbf{F}_i^R$ [26], where m is the monomer mass, ξ the friction coefficient, and $\mathbf{F}_i^R$ the random force, that satisfies the fluctuation-dissipation theorem. The external force is expressed as $\mathbf{F}_{\text{ext}} = F\hat{x}$, where F is the external force strength exerted on the monomers in the pore, and $\hat{x}$ is a unit vector in the direction along the pore axis. In the present work, we use the LJ parameters ε and σ, and the monomer mass m to fix the energy, length and mass scales. This sets the time scale $t_{LJ} = (m\sigma^2/\varepsilon)^{1/2}$. The dimensionless parameters in our simulations are $R_0 = 2$, $k = 7$, $k_BT = 1.2$ and $\xi = 0.7$, unless otherwise stated. The Langevin equation is integrated in 3D by a method described in ref. [27]. Initially, the first monomer of the chain is placed in the entrance of the pore, while the remaining monomers evolve in the Langevin thermostat to obtain an equilibrium configuration. The translocation time is defined as the time interval between the entrance of the first segment into the pore and the exit of the last segment. Typically, we average our data over 1000 independent runs.

We note that in our model hydrodynamic interactions and the polymer-pore interactions are neglected. Regarding the issue of hydrodynamics, recent Molecular Dynamics [28] and Lattice Boltzmann [29,30] results show that hydrodynamics is screened out in a narrow pore, which is the case studied here as well as in the experiments.
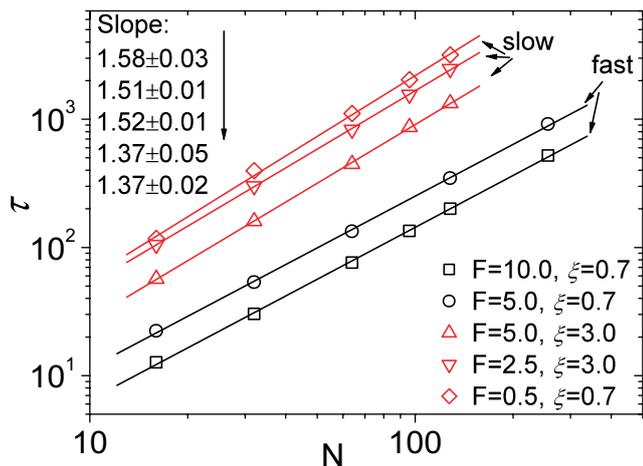
Fig. 2: (Colour on-line) Translocation time τ vs. chain length N for different driving forces F and friction coefficients ξ. For fast translocation (low driving force or high friction) $\alpha \approx 1.37$; for slow translocation $\alpha \approx 1+\nu$.

In ref. [31], however, minor increases of scaling exponents with increasing driving force are obtained in the presence of hydrodynamic interactions. Recently, we have used LD simulations to investigate the influence of an attractive component of polymer-pore interactions on the translocation dynamics [25]. We found that with increasing strength of the attractive interaction, the histogram for the translocation time τ shows a transition from a Gaussian distribution to a long-tailed distribution corresponding to thermal activation over a free-energy barrier. In addition, a strong attractive polymer-pore interaction can directly affect the effective scaling exponents of τ both with N and with the applied voltage, which provides a possible explanation for the different experimental findings on these physical quantities. However, our main focus here is to arrive at a detailed understanding of the translocation dynamics for a purely repulsive pore, and to compare with the results in refs. [22,23] to settle the controversies regarding the scaling behavior of translocation time versus the length of the polymer. Hence, the attractive part of the polymer-pore interaction is left out in this study.

Results and discussion. – As defined above, our pore length is σ and the pore diameter is 2σ. Previous studies [16] showed that for longer pores there is no obvious power-law scaling for relatively short chains. This may be the reason for a linear dependence reported in ref. [32] where the pore length is 5σ with chain length $N < 80$ and in ref. [33] where the pore length is 12σ with chain length $N < 100$. Various heuristic scaling arguments for τ have been presented for short pores, e.g., in refs. [15,16,22,23,34] and will be compared to our numerical results below.

The translocation time as a function of the polymer length is plotted in fig. 2. One of the main features is that α depends significantly on both driving force and friction. For stronger driving forces ($F = 10.0$ and 5.0)

and lower friction ($\xi = 0.7$), we find $\alpha = 1.37 \pm 0.02$ and $\alpha = 1.37 \pm 0.05$, which are in agreement with previous results [18,19,35] and the recent experimental findings for individual short DNA molecules in the range 150–3500 bps through solid-state nanopores [6]. However, decreasing F or increasing ξ, we observe $\alpha = 1.58 \pm 0.03$, 1.51 ± 0.01 and 1.52 ± 0.01 for $F = 0.5$ and $\xi = 0.7$, $F = 2.5$ and $\xi = 3.0$, and $F = 5.0$ and $\xi = 3.0$, respectively. These exponents are in good agreement, not only with the prediction $1 + \nu$ from refs. [15,34], but also with the results from the exact numerical method reported in ref. [21] for low fields, as well as with our previous 2D simulations for relatively long polymers [12,16,17]. These observations demonstrate that there exist two limiting dynamic regimes as demonstrated in fig. 2: slow and fast translocation. For slow translocation, $\alpha \approx 1 + \nu$, while $\alpha \approx 1.37$ for fast translocation.

In the scaling arguments presented in ref. [15], an essential assumption is that the chain is not severely deformed during translocation, and in particular the chain configuration of the already translocated part of the chain is close to equilibrium. For slow translocation, these assumptions are satisfied. Thus, it is not surprising that the predicted exponent $1 + \nu$ is observed in this regime, in contrast to the fast dynamics regime claimed in ref. [20]. Conversely, for fast translocation the chain is highly deformed and the translocation dynamics is different. In our previous 2D simulations based on FB [16] and LD [12,17], a crossover from $\tau \sim N^{2\nu}$ for relatively short polymers ($N < 200$) to $\tau \sim N^{1+\nu}$ for longer chains was found under a stronger driving force $F = 5$ and friction $\xi = 0.7$. Increasing N also slows down the translocation dynamics and thus the system changes from the fast to the slow translocation regime. However, for the same F and ξ values we failed to observe a similar crossover for $N = 40 \sim 800$ in 3D [19], possibly due to the fact that the value of N for the crossover is at a much higher value as compared to the 2D situation. To actually observe the crossover, an alternative choice is to lower the driving force or increase the friction.

Based on the fractional Fokker-Planck equation involving long-range memory effects (compare ref. [36]), the scaling $\alpha = 2\nu + 1 - \gamma_1$ was obtained, such that $\alpha = 1.55$ in 2D and 1.5 in 3D; here γ_1 (≈ 0.945 2D and ≈ 0.68 in 3D) is the critical surface exponent [23]. The MC simulations in ref. [23] were carried out for weak driving forces, producing $\tau \sim N^{1.5}/F$ in 3D, in excellent agreement with the value $\tau \sim N^{1+\nu}/F$ for slow translocation processes. Moreover, using linear response theory with memory effects [24], Vocks et al. [22] came up with an alternative estimate $\tau \sim N^{\frac{1+2\nu}{1+\nu}}$ for 3D, which means $\alpha = 1.37$ in 3D. Their α in 3D is consistent with our numerical data for fast translocation. However, their estimate fails to capture the scaling exponent for slow translocation.

For the driven translocation experiments with a voltage applied across the pore, the force F acts only on the

Table 1: Summary of numerical results. Here, F is the driving force, ξ the friction coefficient, α the scaling exponent of translocation time τ as a function of the chain length N, δ the scaling exponent of translocation velocity as a function of N, and β the scaling exponent of the translocation coordinate s as a function of time. These results clearly demonstrate two regimes.

	F	ξ	F/ξ	α ($\tau \sim N^\alpha$)	δ ($v \sim N^\delta$)	β ($\langle s(t) \rangle \sim t^\beta$)	$\alpha\beta$
Fast translocation	10.0	0.7	14.28	1.37 ± 0.02	-0.79 ± 0.01	0.84 ± 0.01	1.15
	5.0	0.7	7.14	1.37 ± 0.05	-0.79 ± 0.02	0.85 ± 0.01	1.16
Slow translocation	5.0	3.0	1.67	1.52 ± 0.01	-0.94 ± 0.01	0.71 ± 0.01	1.08
	2.5	3.0	0.83	1.51 ± 0.02	-0.95 ± 0.02	0.69 ± 0.01	1.04
	0.5	0.7	0.71	1.58 ± 0.03	-1.01 ± 0.02	0.64 ± 0.01	1.01
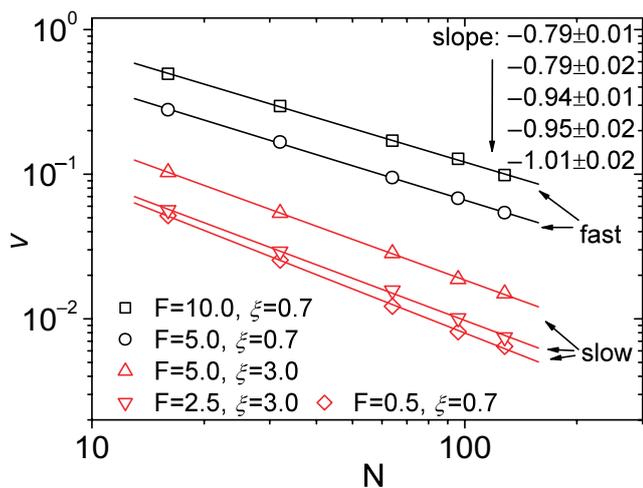
Fig. 3: (Colour on-line) Scaling of translocation velocity with chain length.

Fig. 4: Translocation time τ *vs.* driving force at $\xi = 0.7$. The solid line shows the empirical fitting function for the data, as discussed in the text.

few monomers inside the pore. As a consequence, it was argued [15] that the center of mass of polymer should move with a velocity $v \sim F/N$. Thus the lower bound for the translocation time of an unhindered polymer is the time to move through a distance R_g (radius of gyration of the polymer), giving rise to the scaling $\tau \sim R_g/v \sim N^{1+\nu}/F$. Figure 3 shows the translocation velocity v as function of the polymer length for different driving forces and friction coefficients, $v \sim N^\delta$. Here v is the average velocity with respect to the last monomer (for details see ref. [16]), and we checked that the corresponding v of the center of mass scales in the same way. For slow translocation, we find $\delta = -1.01 \pm 0.02$ for $F = 0.5$ and $\xi = 0.7$, $\delta = -0.95 \pm 0.02$ for $F = 2.5$ and $\xi = 3.0$, and $\delta = -0.94 \pm 0.01$ for $F = 5.0$ and $\xi = 3.0$, which are in good agreement with $v \sim N^{-1}$. For fast translocation the velocity decreases less rapidly with N: $\delta = -0.79 \pm 0.01$ for $F = 10.0$ and $\xi = 0.7$ and $\delta = -0.79 \pm 0.02$ for $F = 5.0$ and $\xi = 0.7$, as observed in ref. [18]. Based on the values of F/ξ we roughly distinguish the slow and fast regimes, see table 1. For fast translocation with $\xi = 0.7$, $F/\xi = 14.28$ for $F = 10.0$ and $F/\xi = 7.14$ for $F = 5.0$, which are much higher than those for the slow translocation where $F/\xi = 0.71$ for $F = 0.5$ and $\xi = 0.7$, $F/\xi = 0.83$ for $F = 2.5$ and $\xi = 3.0$, and $F/\xi = 1.67$ for $F = 5.0$ and $\xi = 3.0$.
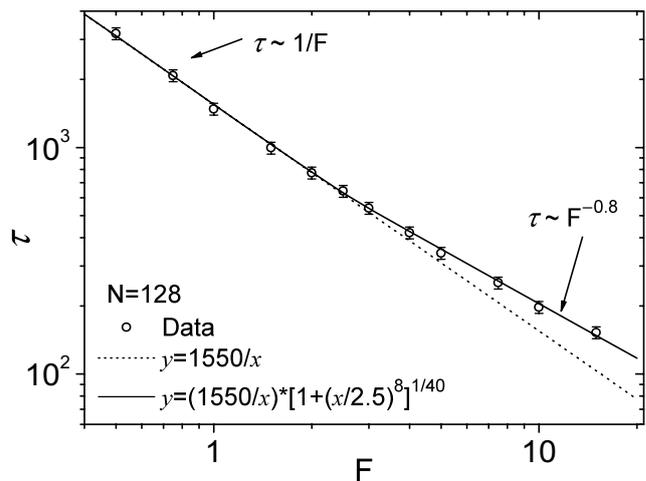
Following the change of the scaling exponent α, the scaling of the average velocity changes from $v \sim N^{-0.79}$ for fast translocation, to $v \sim N^{-1}$ in the case of slow translocation. Furthermore, we have also studied how the translocation time varies as a function of the driving force for $\xi = 0.7$ and $N = 128$ (fig. 4). As long as $F \leqslant 2$ we observe $\tau \sim 1/F$, before crossing over to $\tau \sim F^{-0.80}$ for strong driving. The data can be fitted with an empirical function $\tau = 1550 F^{-1} [1 + (F/2.5)^8]^{1/40}$, yielding the details of the crossover from the slow translocation (weak force) to the fast translocation (strong force) regime for this case. The seemingly high exponent 8 in the empirical function is necessary to account for the relatively fast turnover between the scaling $\tau \sim F^{-1}$ at low force and the behavior $\tau \sim F^{-0.8}$ at high force. The difference of the translocation dynamics in the two regimes can be understood by inspecting the polymer configurations during the translocation process. For faster translocation, only part of the chain on the cis side can respond immediately, while the remaining part near the chain end does not feel the force yet. As a result, a part of the chain on the cis side is deformed to a trumpet and even stem-and-flower shaped [35], while the translocated portion on the trans side has a compact spherical shape, as it does not have time to diffuse away from the pore exit, see fig. 5. With increasing time, the
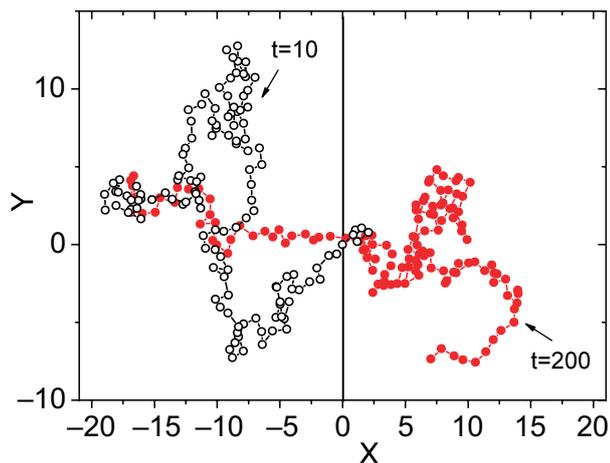
Fig. 5: (Colour on-line) Typical chain conformation during fast translocation for $N = 128$, $\xi = 0.7$, and $F = 5.0$. 3D conformations are projected onto the XY plane. Black: early stage. Red: later stage.
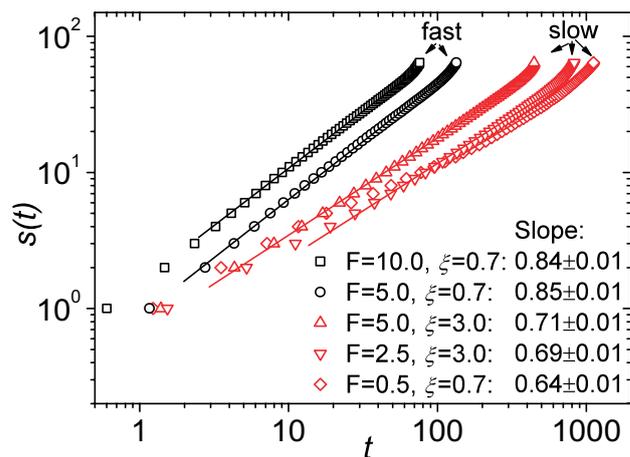

Fig. 7: (Colour on-line) The translocation coordinate (s-coordinate) as a function of time for different driving forces and friction coefficients, for $N = 64$.
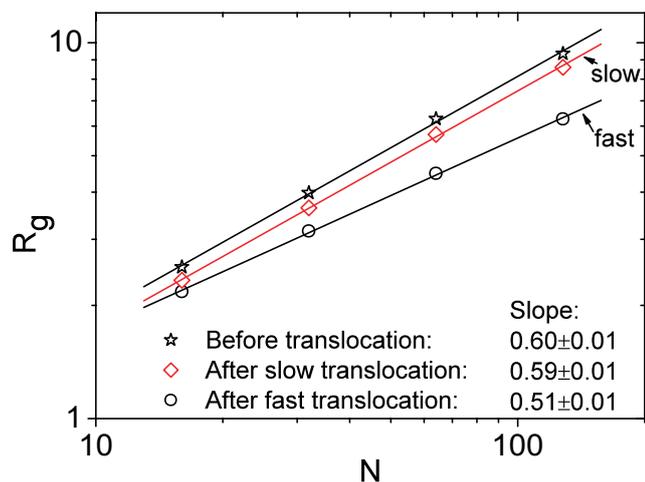

Fig. 6: (Colour on-line) The radius of gyration (R_g) before translocation and at the moment just after the fast translocation ($\xi = 0.7$ and $F = 5.0$), and the slow translocation ($\xi = 0.7$ and $F = 0.5$).

tension propagates along the chain, which changes the chain conformation progressively. Thus, the chain cannot achieve a steady state with average velocity $v \sim N^{-1}$ even in the late stage of the translocation process. Figure 6 shows the radius of gyration (R_g) at the moment just after translocation. For fast translocation, this obeys the scaling behavior $R_g \sim N^{0.51}$, significantly different from the equilibrium scaling of $R_g \sim N^{0.6}$, indicating a non-equilibrium compactification of the chain immediately after translocation. On the other hand, the corresponding scaling behavior for the chain after slow translocation is approximately the same as the chain in equilibrium.

We note that in a recent theoretical study the effect of a trumpet shape of the chain on the cis side, on the translocation dynamics was found to cause a breakdown

of the $\tau \sim 1/F$ scaling [35]. However, this theory neglects effects due to the compacted chain structure on the trans side.

We also checked the translocation coordinate $\langle s(t) \rangle \sim t^\beta$ for $N = 64$ for different F and ξ, see fig. 7 and table 1. For fast translocation with $\xi = 0.7$, we find $\beta = 0.84$ and 0.85 for $F = 10.0$ and 5.0, respectively. However, for slow translocation $\beta = 0.71$ for $F = 5.0$ and $\xi = 3.0$, $\beta = 0.69$ for $F = 2.5$ and $\xi = 3.0$, and $\beta = 0.64$ for $F = 0.5$ and $\xi = 0.7$. Different β values for fast and slow translocation processes demonstrate the existence of different dynamic regimes. The definition $\langle s(t) \rangle \sim t^\beta$ implies that $N \sim \tau^\beta$. Compared with $\tau \sim N^\alpha$, one obtains $\alpha\beta = 1$. For $F = 0.5$ and $\xi = 0.7$, $\alpha\beta = 1.01 \approx 1$, which indicates that non-equilibrium effect does not seem to be severe. However, $\alpha\beta = 1.16$ for $F = 5.0$ and $\xi = 0.7$ indicating a breakdown of "simple" scaling due to highly non-equilibrium effect.

Conclusions. – We have investigated the dynamics of driven polymer translocation through nanopores by 3D Langevin dynamics simulations, focusing on the scaling of the average translocation time τ as a function of the polymer length N. For slow translocation, i.e., under low driving forces and/or high friction, we find $\tau \sim N^\alpha$ with $\alpha \approx 1 + \nu$. In the opposite case, we obtain $\alpha \approx 1.37$. As a function of the driving force F, the dependence $\tau \sim 1/F$ and $\tau \sim F^{-0.80}$ are obtained, respectively, for slow and fast translocation. The different behavior in the two regimes can be understood from analysis of the chain conformations during the translocation process. In the slow translocation case, the configurations at all times are close to the equilibrium case while for the fast translocation regime, there exist highly deformed, unrelaxed chain conformations throughout the translocation process. These results clarify the controversy on the value of α for driven translocation in the existing literature.

* * *

REFERENCES

[1] Alberts A., Bray D., Lewis J., Raff M. and Watson J. D., *Molecular Biology of the Cell* (Garland, New York) 1994.

[2] Meller A., *J. Phys.: Condens. Matter*, **15** (2003) R581.

[3] Kasianowicz J. J., Brandin E., Branton D. and Deamer D. W., *Proc. Natl. Acad. Sci. U.S.A.*, **93** (1996) 13770.

[4] Meller A., Nivon L. and Branton D., *Phys. Rev. Lett.*, **86** (2001) 3435.

[5] Storm A. J., Storm C., Chen J., Zandbergen H., Joanny J.-F. and Dekker C., *Nano Lett.*, **5** (2005) 1193.

[6] Wanunu M., Suntin J., McNally B., Chow A. and Meller A., *Biophys. J.*, **95** (2008) 4716.

[7] Sung W. and Park P. J., *Phys. Rev. Lett.*, **77** (1996) 783.

[8] Muthukumar M., *J. Chem. Phys.*, **111** (1999) 10371.

[9] Chuang J., Kantor Y. and Kardar M., *Phys. Rev. E*, **65** (2001) 011802.

[10] de Gennes P.-G., *Scaling Concepts in Polymer Physics* (Cornell University, Ithaca, New York) 1979; Doi M. and Edwards S. F., *The Theory of Polymer Dynamics* (Clarendon, Oxford) 1986.

[11] Luo K., Ala-Nissila T. and Ying S. C., *J. Chem. Phys.*, **124** (2006) 034714.

[12] Huopaniemi I., Luo K., Ala-Nissila T. and Ying S. C., *J. Chem. Phys.*, **125** (2006) 124901.

[13] Wei D., Wang W., Jin X. and Liao Q., *J. Chem. Phys.*, **126** (2007) 204901.

[14] Milchev A., Binder K. and Bhattacharya A., *J. Chem. Phys.*, **121** (2004) 6024.

[15] Kantor Y. and Kardar M., *Phys. Rev. E*, **69** (2004) 021806.

[16] Luo K., Huopaniemi I., Ala-Nissila T. and Ying S. C., *J. Chem. Phys.*, **124** (2006) 114704.

[17] Luo K., Ala-Nissila T., Ying S. C. and Bhattacharya A., *J. Chem. Phys.*, **126** (2007) 145101.

[18] Bhattacharya A., Morrison W. H., Luo K., Ala-Nissila T., Ying S. C., Milchev A. and Binder K., *Eur. Phys. J. E*, **29** (2009) 423.

[19] Luo K., Ollila S. T. T., Huopaniemi I., Ala-Nissila T., Pomorski P., Karttunen M., Ying S. C. and Bhattacharya A., *Phys. Rev. E*, **78** (2008) 050901(R).

[20] Lehtola V. V., Linna R. P. and Kaski K., *Phys. Rev. E*, **78** (2008) 061803.

[21] Gauthier M. G. and Slater G. W., *J. Chem. Phys.*, **126** (2007) 145101.

[22] Vocks H., Panja D., Barkema G. T. and Ball R. C., *J. Phys.: Condens. Matter*, **20** (2008) 095224.

[23] Dubbeldam J. L. A., Milchev A., Rostiashvili V. G. and Vilgis T. A., *EPL*, **79** (2007) 18002.

[24] Dubbeldam J. L. A., Milchev A., Rostiashvili V. G. and Vilgis T. A., *J. Phys.: Condens. Matter*, **21** (2009) 098001.

[25] Luo K., Ala-Nissila T., Ying S. C. and Bhattacharya A., *Phys. Rev. Lett.*, **99** (2007) 148102; **100** (2008) 058101; *Phys. Rev. E*, **78** (2008) 061911; **78** (2008) 061918.

[26] Allen M. P. and Tildesley D. J., *Computer Simulation of Liquids* (Clarendon, Oxford) 1987.

[27] Ermak D. L. and Buckholz H., *J. Comput. Phys.*, **35** (1980) 169.

[28] Gauthier M. G. and Slater G. W., *Eur. Phys. J. E*, **25** (2008) 17; Guillouzic S. and Slater G. W., *Phys. Lett. A*, **359** (2006) 261.

[29] Lzmitli A., Schwartz D. C., Graham M. D. and de Pablo J. J., *J. Chem. Phys.*, **128** (2008) 085102.

[30] Fyta M., Melchionna S., Succi S. and Kaxiras E., *Phys. Rev. E*, **78** (2008) 036704.

[31] Lehtola V. V., Linna R. P. and Kaski K., *EPL*, **85** (2009) 58006.

[32] Tian P. and Smith G. D., *J. Chem. Phys.*, **119** (2003) 11475.

[33] Paun V. P., *Cent. Eur. J. Phys.*, **7** (2009) 607.

[34] Grosberg A. Yu., Nechaev S., Tamm M. and Vasilyev O., *Phys. Rev. Lett.*, **96** (2006) 228105.

[35] Sakaue T., *Phys. Rev. E*, **76** (2007) 021803.

[36] Metzler R. and Klafter J., *Phys. Rep.*, **339** (2000) 1; see also *Biophys. J.*, **85** (2003) 2776.